Available online at http://ijim.srbiau.ac.ir/
Int. J. Industrial Mathematics (ISSN 2008-5621)
Vol. 10, No. 4, 2018 Article ID IJIM-00802, 14 pages
Research Article

Numerical Study of Coupled Fluid Flow and Heat Transfer in a Rectangular Domain at Moderate Reynolds Numbers using the Control Volume Method

V. Ambethkar *†, M. K. Srivastava ‡, A. J. Chamkha §

Received Date: 2015-12-22 Revised Date: 2016-10-23 Accepted Date: 2017-03-04

Abstract

In this paper, we have used a control volume method to investigate the problem of a fully coupled fluid flow with heat transfer in a rectangular domain with slip wall boundary conditions. We have used this method to solve the governing equations and thereby to compute the convective and diffusive fluxes at the cell faces of the control volumes considered around the grid points of computational domain. We have used a staggered grid approach for the discretization of the governing equations. A SIMPLE algorithm was used for the discretized equations in order to compute the numerical solutions of the flow variables: velocity, pressure and temperature for moderate Reynolds numbers in the range of 500-2500. We have executed this with the aid of a computer program developed and run in C-compiler. Also investigated was the behavior of flow variables for Reynolds numbers $(\Re) = 500, 1000, 1500, 2000, 2500$ and Prandtl number $(\Pr) = 7.00$. The phenomenon inside the rectangular domain was also analyzed for the streamlines and isotherm patterns for moderate Reynolds numbers range. The numerical results have been obtained with desired accuracy.

Keywords : Control volume method; Heat transfer; Isotherms; Prandtl number; Reynolds number; SIMPLE algorithm; Staggered grid; Stream lines.

Nomenclature

x, y	dimensionless Cartesian coordinates
$\Delta x, \Delta y$	dimensionless grid spacing
u, v	dimensionless velocity components
u^*, v^*	initial guess for dimensionless velocity components
P	dimensionless pressure
P^*	initial guess for dimensionless pressure
P'	pressure correction for dimensionless pressure
T	dimensionless temperature
T^*	initial guess for dimensionless temperature
$\Re$	Reynolds number
$\Pr$	Prandtl number

*Corresponding author. vambethkar@gmail.com, Tel: +011-27666658
†Department of Mathematics, University of Delhi, Delhi 110007, India.
‡Department of Mathematics, University of Delhi, Delhi 110007, India.
§Mechanical Engineering Department, Prince Mohammad Bin Fahd University, Al-Khobar 31952, Kingdom of Saudi Arabia.

Table 1: Numerical solutions of u-velocity curves along the vertical line through geometric center of the rectangular domain.

y	u ($\Re = 500$)	u ($\Re = 1000$)	u ($\Re = 1500$)	u ($\Re = 2000$)	u ($\Re = 2500$)
0.0278	0.01068	0.02274	0.02746	0.02892	0.03081
0.0833	-0.00099	0.02300	0.03073	0.03540	0.01748
0.1389	-0.04468	-0.03222	-0.04216	-0.04289	-0.06065
0.1944	-0.09895	0.09135	-0.09079	-0.08285	-0.09156
0.2500	-0.14185	-0.12344	-0.11341	-0.10133	-0.10428
0.3056	-0.16548	-0.13576	-0.12054	-0.10671	-0.10533
0.3611	-0.17096	-0.13502	-0.11721	-0.10324	-0.09858
0.4167	-0.16320	-0.12535	-0.10677	-0.09377	-0.08669
0.4722	-0.14656	-0.10971	-0.09167	-0.08035	-0.07156
0.5278	-0.12419	-0.09035	-0.07374	-0.06455	-0.05465
0.5833	-0.09854	-0.06903	-0.05446	-0.04762	-0.03713
0.6389	-0.07160	-0.04717	-0.03502	-0.03056	-0.01996
0.6944	-0.04445	-0.02583	-0.01617	-0.01405	-0.00286
0.7500	-0.01233	-0.00422	0.00347	0.00319	0.01519
0.8056	0.03791	0.01963	0.02462	0.02179	0.03333
0.8611	0.13983	0.06535	0.04750	0.04058	0.05097
0.9167	0.35592	0.22131	0.15764	0.11717	0.10006
0.9722	0.73943	0.63742	0.57051	0.52089	0.48539

Table 2: Numerical solutions of v-velocity curves along the horizontal line through geometric center of the rectangular domain.

x	v ($\Re = 500$)	v ($\Re = 1000$)	v ($\Re = 1500$)	v ($\Re = 2000$)	v ($\Re = 2500$)
0.0833	0.01651	-0.00684	-0.01552	-0.01854	-0.02009
0.2500	0.00905	-0.00537	-0.00952	-0.01134	-0.01219
0.4167	0.01545	0.00351	-0.00034	-0.00275	-0.00363
0.5833	0.01935	0.01006	0.00725	0.00505	0.00489
0.7500	0.02353	0.01686	0.01507	0.01328	0.01400
0.9167	0.03084	0.02700	0.02592	0.02406	0.02574
1.0833	0.04359	0.04244	0.04142	0.03869	0.04146
1.2500	0.06274	0.06270	0.06132	0.05724	0.06056
1.4167	0.08627	0.08536	0.08253	0.07656	0.07938
1.5833	0.10927	0.10498	0.09931	0.09115	0.09199
1.7500	0.12459	0.11469	0.10561	0.09554	0.09306
1.9167	0.12454	0.10886	0.09712	0.08661	0.07952
2.0833	0.10325	0.08406	0.07100	0.06234	0.05144
2.2500	0.05677	0.03994	0.02885	0.02436	0.01498
2.4167	-0.00615	-0.01293	-0.01602	-0.01480	-0.01794
2.5833	-0.08044	-0.06194	-0.05303	-0.04363	-0.04567
2.7500	-0.21699	-0.16577	-0.14007	-0.11963	-0.11452
2.9167	-0.52218	-0.44759	-0.40090	-0.36422	-0.34298

F_w, F_e convective mass flux per unit area at west and east faces respectively, $\mathrm{kgm^{-2}s^{-1}}$

F_s, F_n convective mass flux per unit area at south and north faces respectively, $\mathrm{kgm^{-2}s^{-1}}$

D_w, D_e diffusivity conductance at west and east faces respectively, $\mathrm{Wm^{-2}K^{-1}}$

D_s, D_n diffusivity conductance at south and north faces respectively, $\mathrm{Wm^{-2}K^{-1}}$

Table 3: Numerical solutions of $\left(\frac{-\partial P}{\partial x}\right)$ along the horizontal linethrough geometric center of the rectangular domain

x	$\Re = 500$	$\Re = 1000$	$\Re = 1500$	$\Re = 2000$	$\Re = 2500$
0.2500	0.00646	0.00450	0.00390	0.00358	0.00314
0.4167	0.00429	0.00336	0.00297	0.00285	0.00254
0.5833	0.00323	0.00214	0.00165	0.00147	0.00122
0.7500	0.00213	0.00101	0.00039	0.00006	-0.00016
0.9167	0.00091	-0.00017	-0.00072	-0.00099	-0.00114
1.0833	0.00001	-0.00085	-0.00114	-0.00143	-0.00117
1.2500	0.00186	0.00131	0.00128	0.00077	0.00177
1.4167	0.01109	0.01020	0.00985	0.00800	0.00994
1.5833	0.03155	0.02797	0.02539	0.02087	0.02295
1.7500	0.06181	0.05132	0.04444	0.03635	0.03727
1.9167	0.09173	0.07150	0.05914	0.04721	0.04554
2.0833	0.10440	0.07540	0.05913	0.04492	0.04059
2.2500	0.08032	0.05317	0.03823	0.02810	0.02223
2.4167	0.02341	0.01048	0.00449	0.00425	-0.00079
2.5833	-0.03978	-0.02448	-0.01886	-0.01365	-0.01468
2.7500	-0.11306	-0.06056	-0.04179	-0.02600	-0.02755
2.9167	-0.18831	-0.12537	-0.09327	-0.08623	-0.06848

Subscript	i, j	index used in tensor notation
	nb	neighboring coordinate
P	central grid point	
E	neighbor in east direction	
W	neighbor in west direction	
N	neighbor in north direction	
S	neighbor in south direction	
e	control volume face P and E	
w	control volume face P and W	
n	control volume face P and N	
s	control volume face P and S	

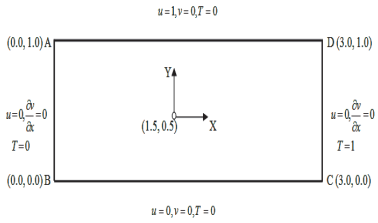

Figure 1: The rectangular domain.

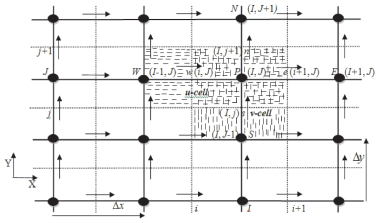

Figure 2: The staggered grid.

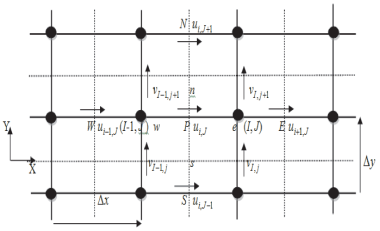

Figure 3: A u-control volume and its neighboring velocity components.

1 Introduction

The problem of coupled fluid flow with heat transfer in a rectangular domain plays an important role in various equipment and process of the industry. For example, there is a direct relevance of coupled fluid flow with heat transfer to a large number of practical applications including feedback control of turbulence for drag reduction, suppression of fluid mechanical instabilities in coating processes, and suppression of instabilities exhibited by falling liquid films, flight tests, flow simulation and residence times in UV-disinfection systems, hygienic design of flow installations in the food indus-

Table 4: Numerical solutions of $\left(\frac{-\partial P}{\partial y}\right)$ along the vertical linethrough geometric center of the rectangular domain

y	$\Re = 500$	$\Re = 1000$	$\Re = 1500$	$\Re = 2000$	$\Re = 2500$
0.0833	-0.00859	-0.00502	-0.00363	-0.00247	-0.00294
0.1389	-0.00585	-0.00316	-0.00172	-0.00093	-0.00068
0.1944	-0.00576	-0.00212	-0.00033	0.00092	0.00102
0.2500	-0.00513	-0.00099	0.00134	0.00227	0.00353
0.3056	-0.00546	0.00007	0.00253	0.00271	0.00462
0.3611	-0.00593	-0.00004	0.00236	0.00210	0.00427
0.4167	-0.00783	-0.00167	0.00075	0.00042	0.00274
0.4722	-0.01008	-0.00410	-0.00164	-0.00190	0.00041
0.5278	-0.01287	-0.00711	-0.00464	-0.00432	-0.00230
0.5833	-0.01536	-0.01000	-0.00750	-0.00644	-0.00514
0.6389	-0.01712	-0.01227	-0.00994	-0.00810	-0.00743
0.6944	-0.01751	-0.01383	-0.01165	-0.00920	-0.00949
0.7500	-0.01654	-0.01510	-0.01308	-0.01015	-0.01090
0.8056	-0.01386	-0.01540	-0.01354	-0.01057	-0.01157
0.8611	-0.00938	-0.01251	-0.01239	-0.01020	-0.01063
0.9167	-0.00448	-0.00525	-0.00672	-0.00741	-0.00754
0.9722	-0.00335	-0.00335	-0.00259	-0.00297	-0.00278

Table 5: Numerical solutions of temperature along the horizontal line through geometric center of the rectangular domain

x	T $(\Re = 500)$	T $(\Re = 1000)$	T $(\Re = 1500)$	T $(\Re = 2000)$	T $(\Re = 2500)$
0.0833	0.37827	0.37903	0.37922	0.37927	0.37926
0.2500	0.22938	0.23112	0.23169	0.23192	0.23207
0.4167	0.13557	0.13766	0.13844	0.13881	0.13905
0.5833	0.07944	0.08140	0.08219	0.08258	0.08285
0.7500	0.04709	0.04859	0.04922	0.04956	0.04978
0.9167	0.02933	0.03021	0.03060	0.03081	0.03095
1.0833	0.02068	0.02089	0.02098	0.02103	0.02105
1.2500	0.01818	0.01767	0.01744	0.01729	0.01717
1.4167	0.02058	0.01929	0.01869	0.01831	0.01803
1.5833	0.02796	0.02576	0.02472	0.02406	0.02359
1.7500	0.04154	0.03829	0.03673	0.03574	0.03505
1.9167	0.06396	0.05952	0.05738	0.05603	0.05510
2.0833	0.09975	0.09419	0.09150	0.08981	0.08870
2.2500	0.15654	0.15034	0.14735	0.14549	0.14432
2.4167	0.24723	0.24157	0.23881	0.23710	0.23601
2.5833	0.39238	0.38908	0.38730	0.38620	0.38531
2.7500	0.62024	0.62086	0.62089	0.62100	0.62055
2.9167	0.96094	0.96335	0.96455	0.96544	0.96568

try, heat exchanger, wind loaded structure, internal combustion engine. Since the primary attractive feature of the control volume method is that it is a method to represent and evaluate partial differential equations in the form of algebraic equations. Ghia *et al.* [12] have used the vorticity-stream function formulation of the two-dimensional incompressible Navier-Stokes equations to study the effectiveness of the coupled strongly implicit multigrid (CSI-MG) method in the determination of high-Refine-mesh flow solutions. Mansour and Hamed [17] used implicit procedure for the solution of the incompressible Navier-Stokes equations on a non-staggered

Table 6: Numerical solutions of temperature along the vertical line through geometric center of the rectangular domain

y	T ($\Re = 500$)	T ($\Re = 1000$)	T ($\Re = 1500$)	T ($\Re = 2000$)	T ($\Re = 2500$)
0.0278	0.00216	0.00200	0.00193	0.00188	0.00185
0.0833	0.00643	0.00595	0.00573	0.00557	0.00549
0.1389	0.01051	0.00972	0.00935	0.00910	0.00896
0.1944	0.01427	0.01319	0.01269	0.01235	0.01215
0.2500	0.01759	0.01625	0.01563	0.01521	0.01496
0.3056	0.02034	0.01879	0.01807	0.01759	0.01730
0.3611	0.02243	0.02073	0.01994	0.01943	0.01909
0.4167	0.02378	0.02201	0.02118	0.02065	0.02029
0.4722	0.02437	0.02259	0.02175	0.02122	0.02085
0.5278	0.02418	0.02247	0.02165	0.02115	0.02077
0.5833	0.02324	0.02165	0.02089	0.02042	0.02006
0.6389	0.02160	0.02019	0.01950	0.01908	0.01875
0.6944	0.01932	0.01813	0.01754	0.01718	0.01687
0.7500	0.01650	0.01555	0.01506	0.01477	0.01451
0.8056	0.01324	0.01252	0.01215	0.01193	0.01172
0.8611	0.00963	0.00916	0.00891	0.00875	0.00860
0.9167	0.00583	0.00556	0.00542	0.00533	0.00525
0.9722	0.00194	0.00186	0.00181	0.00178	0.00176

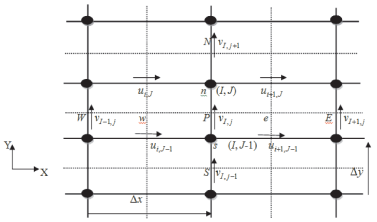

Figure 4: A v-control volume and its neighboring velocity components.

grid. The steady incompressible Navier-Stokes equations in a 2-D driven cavity were solved by Bruneau and Jouron [5] in primitive variables by means of the multigrid method. A finite volume solution method for the two-dimensional Navier-Stokes equations and temperature equation with 4^{th} order discretization on Cartesian grids was presented by Lilek and Peric [16]. Kim and Choi [15] presented a second-order time-accurate numerical method for solving unsteady incompressible Navier-Stokes equations on hybrid unstructured grids. Kalita *et al.* [14] have proposed a higher order compact (HOC) finite difference solution procedure for the steady two-dimensional convection-diffusion equations on non-uniform orthogonal Cartesian grids. Piller and Stalio [20] used the staggered grid arrangement to study one and two-dimensional simulations for the scalar transport and Navier-Stokes equations. Ben-

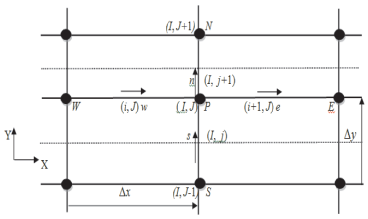

Figure 5: Scalar control volume (continuity equation).

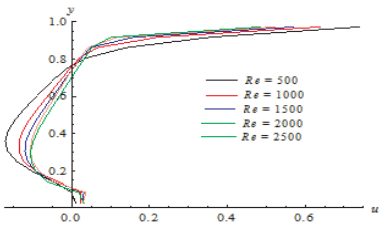

Figure 6: u-velocity curves along the vertical line through geometric center of the domain.

Nakhi and Chamkha [4] studied conjugate natural convection in a square enclosure with inclined thin fin of arbitrary length. Hokpunna and Manhart [13] developed a compact fourth-order finite volume method for solutions of the Navier-

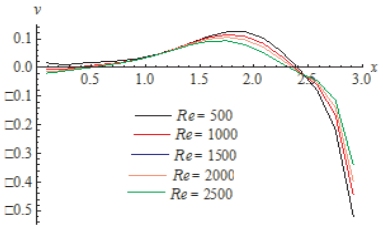

Figure 7: v-velocity curves along the horizontal line through geometric center of the domain.

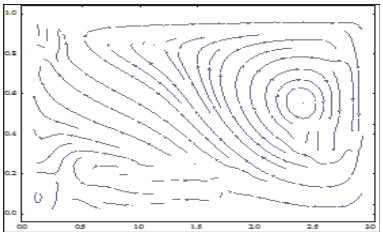

Figure 8: Steady-state contours for stream lines for $\Re = 1000$.

Stokes equations on staggered grids. Basak and Chamkha [3] considered heat line analysis on natural convection for nanofluids confined within square cavities with various thermal boundary conditions. Garoosi et al. [7] reported a study about the natural convection heat transfer of the nanofluid in a square cavity with several pairs of heaters and coolers (HACs) inside.

They found that location of the heater and cooler (HAC) has the highest impact on the heat transfer rate. Chamkha and Ismael [6] analyzed conjugate heat transfer in a porous cavity filled with nanofluids and heated by triangular thick wall. Garoosi et al. [8] studied the natural convection and mixed convection of the nanofluid in a square cavity using Buongiorno model. Garoosi et al. [9] have numerically studied natural convection heat transfer of nanofluid in a 2-D square cavity containing several pairs of heater and coolers (HACs). Garoosi et al. [10] have carried out a numerical study concerning natural and mixed convection heat transfer of nanofluid in a 2-D square cavity with several pairs of heat source-sinks using the finite volume method. Garoosi et al. [11] have used two phase mixture model for numerically investigating the problem of steady state mixed convection heat transfer of nanofluid in a two-sided lid driven cavity with several pairs of heaters and coolers (HACs) inside.

The literature survey pertinent to coupled fluid

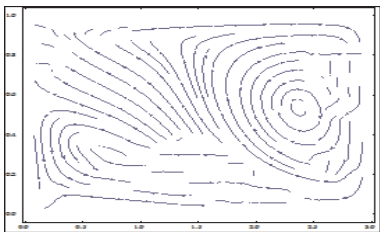

Figure 9: Steady-state contours for stream lines for $\Re = 500$.

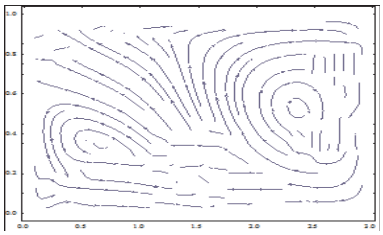

Figure 10: Steady-state contours for stream lines for $\Re = 1500$.

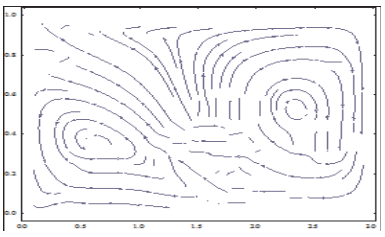

Figure 11: Steady-state contours for stream lines for $\Re = 2000$.

flow with heat transfer in rectangular domain revealed that, to obtain highly accurate numerical solutions of the flow, we need to depend on high accurate and high resolution method like compact control volume method for the present problem. Pressure plays a significant role in predicting the behavior of steady fluid flows. Therefore, we have retained the pressure gradient term for finding the numerical solutions for fluid flow with heat transfer by control volume method. The well-known SIMPLE algorithm is employed for velocity, pressure and temperature coupling. In coupled fluid flow with heat transfer problems, the most important results are to draw the stream lines and isotherms contours inside the rectangular region. The main target of this work is to suitably use the control volume method for solving the problem of

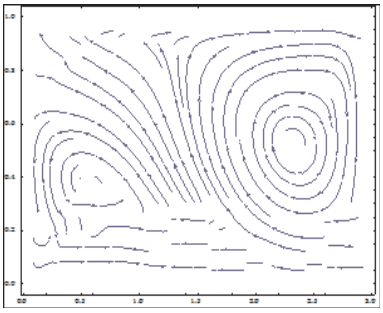

Figure 12: Steady-state contours for stream lines for $\Re = 2500$.

a fully coupled fluid flow with heat transfer in a rectangular domain. We have used this method to solve the governing equations along with slip wall boundary conditions.

The summary of the layout of the current

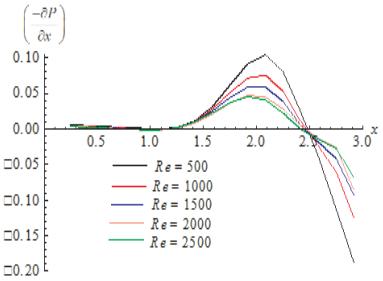

Figure 13: $\left(\frac{-\partial P}{\partial x}\right)$ along the horizontal line through geometric center of the rectangular domain.

work is as follows: Section 2 provides the governing equations of a viscous incompressible fluid flow with heat transfer and the boundary conditions for the rectangular domain. Section 3 describes the control volume method under numerical method. Section 4 describes numerical computations along with the SIMPLE algorithm. Section 5 discusses the numerical solutions of the flow variables, steam lines and isotherms of the flow. Section 6 illustrates the conclusions of this study.

2 Problem Formulation

2.1 Physical Description

The geometry of the problem in the paper along with the boundary conditions is drawn in Fig-

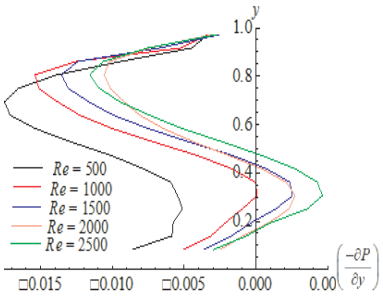

Figure 14: $\left(\frac{-\partial P}{\partial y}\right)$ along the vertical line through geometric center of the rectangular domain.

ure 1. ABCD is a rectangular domain about the point $(1.5, 0.5)$ in which steady 2-D incompressible viscous flow is considered. Flow is setup in a rectangular domain with three stationary walls and a top lid that moves to the right with constant speed ($u = 1$). At all four corner points of the computational domain velocity components are assumed to vanish. It may be noted here regarding specifying the boundary conditions for pressure, the convention followed is that either the pressure at the boundary is given or velocity component normal to the boundary is specified.

2.2 Governing equations

The governing equations of steady 2-D incompressible, viscous fluid flow with heat transfer in a rectangular domain with slip wall boundary conditions are given below. These equations (2.1)-(2.4) subject to boundary conditions (2.5) are discretized using the control volume method. The geometry of the problem in this study along with boundary conditions is drawn in Figure 1. Taking usual Boussinesq approximations into account, the governing equations of the problem in

dimensionless form can be written as follows:

Continuity equation

$$\frac{\partial u}{\partial x}+\frac{\partial v}{\partial y}=0, \tag{2.1}$$

x-momentum equation

$$u\frac{\partial u}{\partial x}+v\frac{\partial u}{\partial y}=-\frac{\partial P}{\partial x}+\left(\frac{1}{\Re}\right)\left(\frac{\partial^2 u}{\partial x^2}+\frac{\partial^2 u}{\partial y^2}\right), \tag{2.2}$$

y-momentum equation

$$u\frac{\partial v}{\partial x}+v\frac{\partial v}{\partial y}=-\frac{\partial P}{\partial y}+\left(\frac{1}{\Re}\right)\left(\frac{\partial^2 v}{\partial x^2}+\frac{\partial^2 v}{\partial y^2}\right), \tag{2.3}$$

Energy equation

$$u\frac{\partial T}{\partial x}+v\frac{\partial T}{\partial y}=\frac{1}{\mathrm{Pr}}\left(\frac{\partial^2 T}{\partial x^2}+\frac{\partial^2 T}{\partial y^2}\right). \tag{2.4}$$

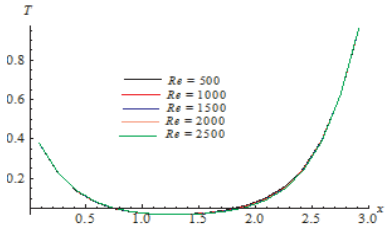

Figure 15: Temperature along the horizontal line through geometric center of the domain.

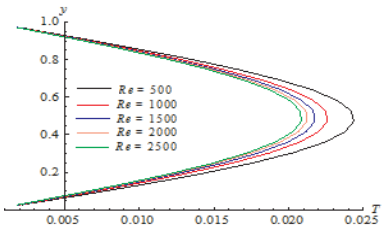

Figure 16: Temperature along the vertical line through geometric center of the domain.

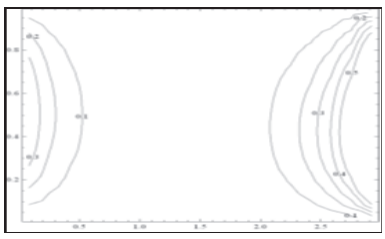

Figure 17: Isotherms for $\Re = 500$.

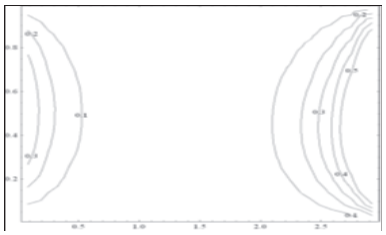

Figure 18: Isotherms for $\Re = 1000$.

2.3 Boundary conditions

The slip wall and temperature boundary conditions are given by:

$$\begin{aligned}
&\text{on boundary AB: } u=0,\ \frac{\partial v}{\partial x}=0, T=0,\\
&\text{on boundary BC: } u=0, v=0, T=0,\\
&\text{on boundary CD: } u=0, \frac{\partial v}{\partial x}=0, T=1,\\
&\text{on boundary AD: } u=1, v=0, T=0.
\end{aligned} \tag{2.5}$$

3 Numerical Method

The numerical method that has been adopted for the problem under study is the Control Volume Method (CVM) based on a uniform staggered grid system. In a staggered grid [21, pp. 195-200] as shown in Figure 2, the scalar variables, including pressure, are stored at the nodes marked (•). The velocities are defined at the (scalar) cell faces in between the nodes and are indicated by arrows. Horizontal arrows indicate the locations for u-velocity and the vertical ones denote those for v-velocity. In addition to the E, W, N, S notation, the u-velocity are stored at cell faces e and w and the v-velocity at cell faces n and s. We observe that the control volumes for u and v are different from the scalar control volumes and from each other. The scalar control volumes are sometimes referred to as the pressure control volumes because the discretized continuity equation is turned into a pressure correction equation, which is evaluated on scalar control volumes.

In Figure 2, the unbroken grid lines are numbered by means of capital letters. In the x-direction the numbering is $\ldots, I-1, I, I+1\ldots$ etc, and in the y-direction the numbering is $\ldots, J-1, J, J+1, \ldots$ etc. The dashed lines that construct the cell faces are denoted by lower case

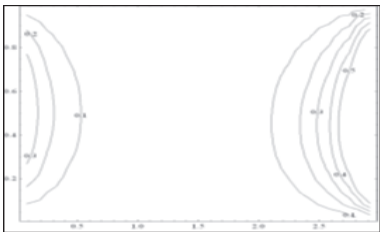

Figure 19: Isotherms for $\Re = 1500$.

letters $\ldots, i-1, i, i+1, \ldots$ and $\ldots, j-1, j, j+1, \ldots$ in the x-and y-directions respectively. A subscript system based on this numbering allows us to define the locations of grid nodes and cell faces with precision. Expressed in the new co-ordinate system, the discretized x-momentum equation at the location (i, J) is given by:

$$a_{i,J}\ u_{i,J} = \Sigma a_{nb} u_{nb} + (P_{I-1,J} - P_{I,J}) A_{i,J}. \quad (3.6)$$

Where $A_{i,J}$is the (east or west) cell face area of

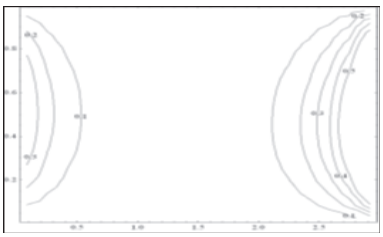

Figure 20: Isotherms for $\Re = 2000$.

the u-control volume. In the numbering system the E, W,N and S neighbors involved in the summation $\Sigma a_{nb} u_{nb}$ are $(i-1, J)$, $(i+1, J)$, $(i, J-1)$ and $(i, J+1)$. Their locations and the prevailing velocities are shown in the Figure 3. The coefficients for hybrid differencing scheme are as follows:

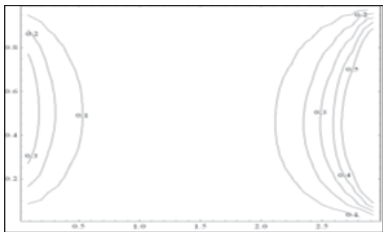

Figure 21: Isotherms for $\Re = 2500$.

$$\begin{aligned}
a_W &= \max\left[F_w, \left(D_w + \frac{F_w}{2}\right), 0\right], \\
a_E &= \max\left[-F_e, \left(D_e - \frac{F_e}{2}\right), 0\right], \\
a_S &= \max\left[F_s, \left(D_s + \frac{F_s}{2}\right), 0\right], \\
a_N &= \max\left[-F_n, \left(D_n - \frac{F_n}{2}\right), 0\right], \\
a_P &= a_W + a_E + a_S + a_N + \Delta F, \\
\Delta F &= (F_e - F_w) + (F_n - F_s).
\end{aligned} \quad (3.7)$$

The coefficients contain combinations of the convective flux F and the diffusive conductance D at u-control volume cell faces. Applying the new notation system we give the values of F and D for each of the faces e, w, n and s of the u-control volume.

$$\begin{aligned}
F_w = (u)_w A_w &= \frac{F_{i,J} + F_{i-1,J}}{2} \\
&= \frac{1}{2}\left[u_{i,J} A_{i,J} + u_{i-1,J} A_{i-1,J}\right], \\
F_e = (u)_e A_e &= \frac{F_{i+1,J} + F_{i,J}}{2} \\
&= \frac{1}{2}\left[u_{i+1,J} A_{i+1,J} + u_{i,J} A_{i,J}\right], \\
F_s = (v)_s A_s &= \frac{F_{I,j} + F_{I-1,j}}{2} \\
&= \frac{1}{2}\left[v_{I,j} A_{I,j} + v_{I-1,j} A_{I-1,j}\right],
\end{aligned}$$

$$\begin{aligned}
F_n = (v)_n A_n &= \frac{F_{I,j+1} + F_{I-1,j+1}}{2} \\
&= \frac{1}{2}\left[v_{I,j+1} A_{I,j+1} + v_{I-1,j+1} A_{I-1,j+1}\right], \\
D_w = \frac{1}{\Re \Delta x},\ D_e &= \frac{1}{\Re \Delta x},\ D_s = \frac{1}{\Re \Delta y}, \\
D_n &= \frac{1}{\Re \Delta y}.
\end{aligned} \quad (3.8)$$

By analogy the y-momentum equation becomes

$$a_{I,j}\ v_{I,j} = \Sigma a_{nb} v_{nb} + (P_{I,J-1} - P_{I,J}) A_{I,j}. \quad (3.9)$$

The neighbors involved in the summation $\Sigma a_{nb} v_{nb}$ and prevailing velocities are as shown in the Figure 4.

The pressure correction equation is given by:

$$a_{I,J}P'_{I,J} = a_{I+1,J}P'_{I+1,J} + a_{I-1,J}P'_{I-1,J} + a_{I,J+1}P'_{I,J+1} + a_{I,J-1}P'_{I,J-1} + b'_{I,J}. \quad (3.10)$$

Where

$$a_{I,J} = a_{I+1,J} + a_{I-1,J} + a_{I,J+1} + a_{I,J-1},$$

$$a_{I+1,J} = (dA)_{i+1,J},$$

$$a_{I-1,J} = (dA)_{i,J},$$

$$a_{I,J+1} = (dA)_{I,j+1},$$

$$a_{I,J} = (dA)_{I,j},$$

$$d_{i,J} = \frac{A_{i,J}}{a_{i,J}}, d_{I,j} = \frac{A_{I,j}}{a_{I,j}}, \quad (3.11)$$

$$b'_{I,J} = (u^*A)_{i,J} - (u^*A)_{i+1,J} + (v^*A)_{I,j} - (v^*A)_{I,j+1}.$$

Finally, the temperature discretized equation

$$a_P T_P = a_W T_W + a_E T_E + a_S T_S + a_N T_N. \quad (3.12)$$

Where

$$a_W = \max\left[F_w, \left(D_w + \frac{F_w}{2}\right), 0\right],$$

$$a_E = \max\left[-F_e, \left(D_e - \frac{F_e}{2}\right), 0\right],$$

$$a_S = \max\left[F_s, \left(D_s + \frac{F_s}{2}\right), 0\right],$$

$$a_N = \max\left[-F_n, \left(D_n - \frac{F_n}{2}\right), 0\right],$$

$$a_P = a_W + a_E + a_S + a_N + \Delta F, \quad (3.13)$$

$$\Delta F = (F_e - F_w) + (F_n - F_s).$$

(3.14)

$$F_w = u_{i,J},\ F_e = u_{i+1,J},$$

$$F_s = v_{I,j},\ F_n = v_{I,j+1},$$

$$D_w = \frac{1}{\mathrm{Pr}\,\Delta x},\ D_e = \frac{1}{\mathrm{Pr}\,\Delta x},$$

$$D_s = \frac{1}{\mathrm{Pr}\,\Delta y},\ D_n = \frac{1}{\mathrm{Pr}\,\Delta y}.$$

4 Numerical Computations

We have obtained the numerical computations of the four unknown flow variables u, v, P, and T by using the discretized equations (3.6), (3.9), (3.10) and (3.12) respectively. The input data, for the relevant parameters in the governing equations like Reynolds number ($\Re$) and Prandtl number (Pr), has been properly chosen by considering physical significance of the present problem. To compute the numerical solutions, we have used the SIMPLE algorithm. We have executed the algorithm with the aid of a computer program developed and run in C-complier. The acronym SIMPLE stands for Semi-Implicit Method for Pressure-Linked Equations. The algorithm is originally put forward by Patankar and Spalding [21] and essentially a guess-and correct procedure for the calculation of pressure on a staggered grid arrangement introduced above. We preferred to use the SIMPLE algorithm that gives a method of calculating pressure and velocities. The method is iterative, and when other scalars are coupled to the momentum equations the calculation needs to be done sequentially. The discretized momentum equations and pressure correction equation are solved implicitly; where the velocity correction is solved explicitly. This is the reason why it is called "Semi-Implicit Method". The algorithm involves aniterative process in which the pressure correction equation is susceptible to divergence unlesssome under-relaxation is used. We have used a suitable under-relaxation factor to find outthe converged values of pressure and velocities.

4.1 The SIMPLE Algorithm

The SIMPLE algorithm for solving coupled fluid flow and heat transfer consists of the following steps:

[Step 1.]Start with guessed velocities u^*, v^*, pressure fields $P^*$and temperature T^*. Calculate the coefficients in the momentum equation, solve discretized momentum equations. Calculate the coefficients of the pressure equation, solve pressure correction equation. Correct pressure and

velocities:

$$\left.\begin{aligned} P_{I,J} &= P^*_{I,J} + P'_{I,J}, \\ u_{i,J} &= u^*_{i,J} + d_{i,J}(P'_{I-1,J} - P'_{I,J}), \\ v_{I,j} &= v^*_{I,j} + d_{I,j}(P'_{I,J-1} - P'_{I,J}). \end{aligned}\right\} \quad (4.15)$$

Solve the temperature discretized equations. Replace the previous intermediate values of pressure and velocity (u^*, v^*, P^*, T^*) **until the corrected values** (u, v, P, T)**return to Step 2 and repeat this process until the solution converges.**

The pressure correction equation (3.10) is also prone to divergence unless some under-relaxation is used. So we underrelax u^*, v^* while solving the momentum equation (with a relaxation factor α), further we employ

$$P_{I,J} = P^*_{I,J} + \alpha_P P'_{I,J}$$

.

5 Numerical Results and Discussion

We have used the control volume method described under section 3 to carry out the numerical computations of velocity, pressure and temperature. We have summarized this method under SIMPLE algorithm described under section 4. In order to get clear insight into the problem, the numerical computations of velocity, pressure gradients and temperature for $\Re = 500, 1000, 1500, 2000, 2500$ and Pr = 7.0 have been done based on the method described under Section 3 along with the algorithm given under Section *4.1*. The behavior of fluid flow variables which are horizontal and vertical components of velocity, pressure gradients and temperature has been described by using the numerical solutions given under Tables 1–6. In Table 1, we list out the numerical solutions for u-velocity curves at different Reynolds numbers ($\Re$ = 500, 1000, 1500, 2000, 2500), along the vertical line through geometric center of the rectangular domain. Its behavior has been illustrated in Figure 6. We observed that, for a given $\Re$, u-velocity first decreases from the bottom boundary ($u = 0$) value and then, gradually increases up to the upper boundary ($u = 1$) value. We also observed that, the absolute value of u-velocity decreases with increase in Reynolds number. The near-linearity of u-velocity curves in the central core of the rectangular domain can also be observed. Similarly, Table 2 shows the numerical solutions for v-velocity curves at different Reynolds numbers ($\Re = 500, 1000, 1500, 2000, 2500$). Figure 7 illustrates the behavior of v-velocity curves along the horizontal line, through the geometric centre of the rectangular domain. It is evident that, for a given $\Re$, v-velocity increases initially and then decreases after attaining its extremum value. Further, the absolute value of v-velocity decreases with increase in Reynolds number. Figures 8-12 display steady-state contours for the stream lines for $\Re = 500, 1000, 1500, 2000, 2500$. The origin for these contours for various Reynolds numbers ($\Re$) has been displayed for clarity of the velocity curves. The recirculating nature of the fully developed flow induced due to the moving upper wall is seen vividly inside the rectangular domain. The point of zero velocity represents the center around which the general body of the fluid rotates in the rectangular domain. This center is located in the direction of the moving boundary. The effect of the velocity of the upper wall on the fluid inside the rectangular domain diminishes as we move away from the upper wall boundary. The numerical solution for $\left(\frac{-\partial P}{\partial x}\right)$ along the horizontal line of the rectangular domain has been given in Table 3. In Figure 13 we illustrate the behavior of $\left(\frac{-\partial P}{\partial x}\right)$ for

$$\Re = 500, 1000, 1500, 2000, 2500$$

. We observed that

$$\left(\frac{-\partial P}{\partial x}\right)$$

is increasing initially and then decreases after attaining its extremum value. In Table 4, the numerical solution for

$$\left(\frac{-\partial P}{\partial y}\right)$$

along the vertical line of the rectangular domain has been presented. Figure 14 illustrates the be-

havior of $\left(\frac{-\partial P}{\partial y}\right)$ for

$$\Re = 500, 1000, 1500, 2000, 2500$$

. We observed that $\left(\frac{-\partial P}{\partial y}\right)$ is increasing near boundaries and decreases inside the domain. We also observed that $\left(\frac{-\partial P}{\partial x}\right)$ and $\left(\frac{-\partial P}{\partial y}\right)$ both decreases with the increment in $\Re$. The numerical solutions of temperature profile, for $\Re = 500, 1000, 1500, 2000, 2500$ and for $\mathrm{Pr} = 7.00$, have been given under Table 5 and 6. Figure 15 illustrates the behavior of T along the horizontal line through the geometric centre of the rectangular domain. Figure 16 illustrates the behavior of T along the vertical line through the geometric centre of the rectangular domain. These figures are depicting a comparison of the heat transfer from the wall CD towards the wall AB and from the wall BC towards the wall AD of the rectangular physical domain considered. The isotherms contours have been drawn to illustrate the fluid flow behavior inside the rectangular domain. It can be observed that high temperature generated at the right and left wall boundaries extended towards the middle of the rectangular domain.

6 Conclusions

The problem of a steady 2-D incompressible, viscous flow with heat transfer with slip wall boundary conditions in a rectangular domain has been investigated. A control volume method, with hybrid scheme has been employed as a numerical scheme to solve the governing equations of this problem. The well-known SIMPLE algorithm is employed for velocity, pressure and temperature coupling. The numerical computations for these flow variables have been obtained by employing the SIMPLE algorithm which has been implemented with the help of a code in C-programming language. In this study, Reynolds numbers $(\Re) = 500, 1000, 1500, 2000, 2500$ have been considered. Prandlt number $(\mathrm{Pr}) = 7.0$, which physically correspond to water, has been consider for this study. We observed that, the absolute value of velocity profile decreases with increase in Reynolds number. The recirculating nature of the fully developed flow induced due to the moving upper wall is seen vividly inside the rectangular domain. The effect of the velocity of the upper wall on the fluid inside the rectangular domain diminishes as we move away from the upper wall boundary. We also observed that $\left(\frac{-\partial P}{\partial x}\right)$ and $\left(\frac{-\partial P}{\partial y}\right)$ both decreases with the increment in $\Re$. The figures, related to temperature profile, are depicting a comparison of the heat transfer from the wall CD towards the wall AB and from the wall BC towards the wall AD of the rectangular physical domain considered. The isotherm contours inside the domain depicted that high temperature generated at the right and left boundaries extended towards the middle of the domain.

Acknowledgements

The authors acknowledge the support from the Research Council, University of Delhi for providing Research and Development Grant 2014-15 vide letter no. RC/2014/6820 to carry out this work.

References

[1] J. D. Anderson, Computational Fluid Dynamics with Basics and Applications, *McGraw-Hill, New York,* 1995.

[2] D. A. Anderson, R. H. Pletcher, J. C. Tannehill, Computational Fluid Mechanics and Heat Transfer, *Second ed., Taylor and Francis, Washington D. C.*, 1997.

[3] T. Basak, A. J. Chamkha, Conjugate natural convection in a square enclosure with inclined thin fin of arbitrary length, *International Journal of Heat and Mass Transfer* 55, 5526-5543 (2012).

[4] A. Ben-Nakhi, A. J. Chamkha, Conjugate natural convection in a square enclosure with inclined thin fin of arbitrary length, *International Journal of Thermal Sciences* 46 (2007) 467-478.

[5] C. H. Bruneau, C. Jouron, An efficient scheme for solving steady incompressible Navier-Stokes equations, *Journal of Computational Physics* 89 (1990) 389-413.

[6] A. J. Chamkha, M. A. Ismael, Conjugate heat transfer in a porous cavity filled with nanofluids and heated by triangular thick wall, *International Journal of Thermal Sciences* 67 (2013) 135-151.

[7] F. Garoosi, G. Bagheri, F. Talebi, Numerical simulation of natural convection of nanofluids in a square cavity with several pairs of heaters and coolers (HACs) inside, *International Journal of Heat and Mass Transfer* 67 (2013) 362-376.

[8] F. Garoosi, S. Garoosi, K. Hooman, Numerical simulation of natural convection and mixed convection of the nanofluid in a square cavity using Buongiorno model, *Powder Technology* 268 (2014) 279-292.

[9] F. Garoosi, L. Jahanshaloo, M. M. Rashidi, A. Badakhsh, M. E. Ali, Numerical simulation of natural convection of the nanofluid in heat exchangers using a Buongiorno model, *Applied Mathematics and Computation* 254 (2015) 183-203.

[10] F. Garoosi, B. Rohani, M. M. Rashidi, Two phase simulation of natural convection and mixed convection of the nanofluid in a square cavity, *Powder Technology* 275 (2015) 239-256.

[11] F. Garoosi, B. Rohani, M. M. Rashidi, Two-phase mixture modeling of mixed convection of nanofluids in a square cavity with internal and external heating, *Powder Technology* 275 (2015) 304-321.

[12] U. Ghia, K. N. Ghia, C. T. Shin, High-resolutions for incompressible flow using the Navier-Stokes equations and a multigrid method, *Journal of Computational Physics* 48 (1982) 387-411.

[13] A. Hokpunna, M. Manhart, Compact fourth-order finite volume method for numerical solutionsof Navier-Stokes equations on staggered grids, *Journal of Computational Physics* 229 (2010) 7545-7470.

[14] J. C. Kalita, A. K. Dass, D. C. Dalal, A transformation-free HOC scheme for steady convection-diffusion on non-uniform grids, *International Journal for Numerical Methods in Fluids* 44 (2004) 33-53.

[15] D. Kim, H. Choi, A second-order time-accurate finite volume method for unsteady incompressible flow on hybrid unstructured grids, *Journal of Computational Physics* 162 (2000) 411-428.

[16] Z. Lilek, M. Peric, A fourth-order finite volume method with collocated variable arrangement, *Computers and Fluids* 24 (1995) 239-252.

[17] M. L. Mansour, A. Hamed, Implicit solution of the incompressible Navier-Stokes equations on non-staggered grid, *Journal of Computational Physics* 86 (1990) 147-167.

[18] S. V. Patankar, Numerical Heat Transfer and Fluid Flow, *Hemisphere, New York*, 1980.

[19] R. Peyret, T. D. Taylor, Computational Methods for Fluid Flow, *Springer-Verlag, New York*, 1983.

[20] M. Piller, E. Stalio, Finite-volume compact schemes on staggered grids, *Journal of Computational Physics* 197 (2004) 299-340.

[21] H. K. Versteeg, W. Malalsekra, An Introduction to Computational Fluid Dynamics: The Finite Volume Method, *Second ed. Pearson, India*, 2007.

V. Ambethkar is Associate Professor, Department of Mathematics, University of Delhi, Delhi. He earned his Ph.D from Osmaina University, Hyderabad in Computational Fluid Mechanics. His area of research interest is Fluid Mechanics, CFD, Heat and Mass Transfer, FDM, FVM, Numerics of PDEs. He is reviewer to several national and international peer reviewed Journals. He published 25 research papers in refereed national and international Journals.

Mohit Kumar Srivastava is Ph.D. in Computational Fluid Dynamics from University of Delhi, India. He earned his M.Sc. (Mathematics) from Indian Institute of Technology Kanpur, India and B.Sc. from University of Allahabad, India. His Research interests include CFD, Numerical Analysis, Numerical solutions of PDEs.

Ali J. Chamkha is the Dean of Research, Professor and former Chairman of the Mechanical Engineering Department and Prince Sultan Endowed Chair for Energy and Environment at Prince Mohammad Bin Fahd University (PMU) in the Kingdom of Saudi Arabia. He earned his Ph.D. in Mechanical Engineering from Tennessee Technological University, USA, in 1989. His research interests include multiphase fluid-particle dynamics, nanofluids dynamics, fluid flow in porous media, heat and mass transfer, magnetohydrodynamics and fluid-particle separation. He has served as an Editor, Associate Editor, or a member of the editorial board for many journals such as ASME Journal of Thermal Science and Engineering Applications, International Journal of Numerical Method for Heat and Fluid Flow, Journal of Nanofluids, Recent Patents on Mechanical Engineering, Journal of Applied Fluid Mechanics, International Journal of Fluids and Thermal Sciences, Journal of Heat and Mass Transfer Research, International Journal for Microscale and Nanoscale Thermal and Fluid Transport Phenomena and many others. He has authored and co-authored over 550 publications in archival international journals and conferences.